Poor Outcome in Estrogen Receptor–Positive Breast Cancers Predicted by Loss of *Plexin B1*

Achim Rody,[1] Uwe Holtrich,[1] Regine Gaetje,[1] Mathias Gehrmann,[4] Knut Engels,[2] Gunter von Minckwitz,[5] Sibylle Loibl,[1] Raihanatou Diallo-Danebrock,[6] Eugen Ruckhäberle,[1] Dirk Metzler,[3] Andre Ahr,[1] Christine Solbach,[1] Thomas Karn,[1] and Manfred Kaufmann[1]

Abstract

Purpose: A common characteristic of mammary carcinomas is an inverse relationship between the estrogen receptor (ER) status and the proliferative activity of the tumor. Yet, a subset of ER-positive breast cancers is characterized by a high proliferation, suggesting malfunctions in ER responsiveness that influence the biological and therapeutic behavior of tumor cells. The expression of several ER-dependent genes seems to be dysregulated among those "uncoupled" tumors. One of those genes is *plexin B1*, a cell-surface receptor for the semaphorin Sema4D (CD 100). However, the biological role of plexin B1 in breast cancer is largely unknown.

Experimental Design: Expression data of plexin B1 were obtained from Affymetrix microarray analysis of $n = 119$ breast cancer specimens. Validation was done by quantitative real-time PCR and protein expression was evaluated by immunohistochemistry. Expression data were compared with clinical characteristics as well as follow-up data of the disease.

Results: Low plexin B1 expression levels characterize a more aggressive tumor phenotype. The expression of plexin B1 is strongly correlated with the ER status. However, even among ER-positive tumors, loss of plexin B1 is associated with an impaired prognosis of breast cancer patients in both univariate (all patients, $P = 0.0062$; ER positive, $P = 0.0107$) and multivariate analyses (all patients, $P = 0.032$; ER positive, $P = 0.022$). Immunohistochemistry reveals that the tumor cells themselves and not the endothelial cells are the major source of plexin B1 expression in the tumor.

Conclusion: Plexin B1 acts not only as a new important prognostic but should also represent a predictive marker indicating an endocrine resistance. These data give a new insight in markers that could be involved in endocrine dysregulation of breast cancer.

Plexins are cell-surface receptors for semaphorin molecules. They have been shown to be widely expressed in various epithelial cells and their interaction governs cell adhesion and migration in a variety of tissues [for recent reviews, see Kruger et al. (1) and Bussolino et al. (2)]. Plexins belong to the c-Met family of scatter factor receptors but lack an intrinsic tyrosine kinase domain. Their ligands, the semaphorins, are cell-surface and secreted proteins and were first identified as repulsive axonal guidance molecules governing neuronal growth. Later on, it was recognized that these ligand receptor pairs regulate cell motility in many cell types. Giordano et al. (3) reported that plexin B1 triggers invasive growth, a complex program that includes cell-cell dissociation, anchorage-independent growth, and branching morphogenesis. Because plexins are broadly expressed, additional biological roles for semaphorin-plexin signaling in development and disease will probably be elucidated. Several groups presented evidence for essential roles for semaphorins in organizing several nonneural tissues like heart (4–6), lung (7), mammary gland (8), and bone homeostasis (9). In addition, autocrine loops of semaphorin-plexin signaling have been suggested to have tumor suppressor function in normal epithelial cells, and loss of heterozygosity of these genes might potentially foster deregulated tumor cell adhesion and migration (10–13). In contrast, because of the observation that plexin B1 couples with the receptor tyrosine kinases Met (3) and ErbB2 (14), it has been speculated that plexin B1 may trigger invasive growth of epithelial cells (3).

To date, there is only limited knowledge about the expression of plexins and semaphorins in breast cancer, their regulation, and their roles in disease prognosis and prediction. We identified *plexin B1* among dysregulated genes in breast cancers with disturbed ER signaling. Here, we show by a combination

Authors' Affiliations: Departments of [1]Obstetrics and Gynecology, [2]Pathology, and [3]Computer Science and Mathematics, Johann Wolfgang Goethe University, Frankfurt, Germany; [4]Bayer Healthcare AG, Leverkusen, Germany; [5]German Breast Group, Neu-Isenburg, Germany; and [6]Department of Pathology, Heinrich Heine-University, Duesseldorf, Germany

Received 10/4/06; revised 11/3/06; accepted 11/7/06.

Grant support: Deutsche Krebshilfe, Bonn, the Margarete Bonifer-Stiftung, Bad Soden, the BANSS-Stiftung, Biedenkopf, and the Dr. Robert Pfleger-Stiftung, Bamberg, Germany.

The costs of publication of this article were defrayed in part by the payment of page charges. This article must therefore be hereby marked *advertisement* in accordance with 18 U.S.C. Section 1734 solely to indicate this fact.

Note: Supplementary data for this article are available at Clinical Cancer Research Online (http://clincancerres.aacrjournals.org/).

Requests for reprints: Thomas Karn, Department of Obstetrics and Gynecology, Johann Wolfgang Goethe University, Theodor-Stern-Kai 7, 60596 Frankfurt, Germany. Phone: 49-69-6301-4120; E-mail: t.karn@em.uni-frankfurt.de.

doi:10.1158/1078-0432.CCR-06-2433

of Affymetrix microarray profiling, quantitative real-time PCR, and immunohistochemical analysis that loss of plexin B1 is a marker for poor prognosis in breast cancer, which was verified on independent published data sets.

Materials and Methods

Breast cancer samples. Tissue samples were obtained from consecutive patients undergoing surgical resection between December 1996 and July 2003 at the Department of Gynecology and Obstetrics at the Johann Wolfgang Goethe University in Frankfurt. Patients were selected for this study if they had received adjuvant chemotherapy (cyclophosphamide-methotrexate-5-fluorouracil or epirubicin-cyclophosphamide) and sufficient follow-up data of more than 2 years were available (n = 119). Patients with positive hormone receptor status received additional tamoxifen for 5 years. All tissue samples were stored in liquid nitrogen. Clinical characteristics of the patients are given in Table 1.

Microarray analysis. Isolation of RNA and expression profiling using Affymetrix Human Genome U133A microarrays was done as described elsewhere (15). Briefly, hybridization intensity data were automatically acquired and processed by Affymetrix Microarray Suite 5.0 software. The expression level of each gene was determined by calculating the average of differences in intensity (perfect match-mismatch) between its probe pairs. Scans were rejected if the scaling factor exceeded 2 or "chip surface scan" revealed scratches, specks, or gradients affecting overall data quality (Refiner, GeneData AG, Basel, Switzerland). The data were subsequently analyzed by using the Cluster and TreeView software package (16). Before cluster analysis, gene chip expression values were adjusted by log transformation and median centering of the gene chips. Hierarchical gene clustering was done by the similarity metric "absolute correlation (centered)."

Assessment of ER, ErbB2, proliferative status, and plexin B1 expression of the samples. Samples were characterized according to standard pathology including the estrogen receptor (ER) status by ligand binding assays or immunohistochemistry. In addition, immunohistochemistry data of the progesterone receptor and ErbB2 were available for most cases. Because differences existed between the two methods used for determining the ER status and data for some samples were missing, the "molecular" status for the receptors was additionally determined based on Affymetrix expression data resulting in concordance of >90%. The molecular ER status was determined using a cutoff value of 1,000 for the Affymetrix probe set 205225_at corresponding to the estrogen receptor gene (*ESR1*), as has been by others (17). Identical results were obtained for 113 of the 119 samples when genes dependent on the ER status described by Gruvberger et al. (18) were used to cluster the samples into two groups. For use as an ordinal variable, the ranking of all samples according to the *ESR1* probe set 205225_at was used. For Affymetrix data on ErbB2 mRNA expression, a cutoff of 4,500 was identified for probe set 216836_s_at by using samples with a 3+ staining in immunohistochemistry with HER2 antibody. This cutoff also correlated very well with the ErbB2-like subtype based on the "intrinsic gene set" of Sorlie et al. (19) as previously shown (20). To obtain a quantitative metric for the molecular proliferation state, we used a cluster of 136 highly correlated genes well known for their association with proliferation (see Supplementary Fig. S9; Supplementary Table S4) similar to the method proposed by Sotiriou et al. (21). For plexin B1 Affymetrix data (probe set 215807_s_at), a cutoff value of 500 was determined by comparison with the ER status (see Results).

Table 1. Correlation of plexin B1 expression with clinical characteristics of breast cancers

	Total, N = 119	Plexin B1 expression (Affymetrix value)		P
		High (>500), n = 54	Low (≤500), n = 65	
Age (y)				
<50	59	33	26	0.027
≥50	60	21	39	
Tumor stage				
1	60	30	30	n.s.
2	49	18	31	
3	4	3	1	
4	6	3	3	
Nodal status				
Negative	66	29	37	n.s.
Positive	51	25	26	
Unknown	2	0	2	
Histology				
Ductal	87	29	58	<0.001
Lobular	25	20	5	
Mixed	3	3	0	
Other	4	2	2	
Molecular grading				
High proliferation	60	15	45	<0.001
Low proliferation	59	39	20	
ER status				
Positive	79	52	27	<0.001
Negative	40	2	38	
HER2 status				
Positive	23	5	18	0.018
Negative	96	49	47	
Molecular subtype				
Basal-like	31	4	27	<0.001
Erbb2-like	20	3	17	
Luminal A	67	46	21	
Luminal B	1	1	0	

Analysis of mRNA expression by quantitative real-time PCR. Total RNA from human primary mammary carcinomas was isolated by the guanidinium isothiocyanate method as described (22) in combination with affinity purification (RNeasy, Qiagen, Hilden, Germany). Real-time PCR analyses were done using the ABI 7700 Sequence Detection System (PE-Applied Biosystems, Foster City, CA). cDNAs were generated by random primed reverse transcription (ProSTAR cDNA-synthesis kit, Stratagene, La Jolla, CA) as previously described (23, 24). PCR reactions were done according to the manufacturer's protocols (PE-Applied Biosystems). VIC-fluorophore–labeled glycerol-3-phosphate dehydrogenase (GPDH) TaqMan probes served as reference quantification markers. Each quantitation was reproduced thrice and normalized to GPDH using the ΔC_t method. Pearson correlation was used to compare the ΔC_t values to Affymetrix microarray data. Primer sequences used for plexin B1 detection were as follows: PlxnB1-U1, 5′-ACCACAAGCTGGGC-CGGGACTCCC-3′; PlxnB1-L1, 5′-GATGTCTGCATAGTACCTTTCCAC-3′.

Immunohistochemical detection of plexin B1 protein expression. Frozen breast cancer tissues were cut into 5-μm sections and placed on superfrost charged slides. Immunohistochemistry was done according to standard procedures. Briefly, the slides were fixed for 10 min in acetone (−20°C) and incubated at room temperature with a primary monoclonal anti–plexin B1 antibody (Santa Cruz Biotechnology, Santa Cruz, CA; 1:100 dilution) for 1 h. Cy3-labeled antimouse secondary antibody (Dianova, Hamburg, Germany) was used to detect plexin B1 by fluorescence. Sections were counterstained with 4′,6-diamidino-2-phenylindole and then mounted with a coverslip. Basic routine H&E staining (modified Schmidt's hematoxylin) was done for all specimens to ensure tissue quality. Staining of the tissues with the anti–plexin B1 antibody was only observed in breast cancers positive for plexin B1 mRNA expression. Furthermore, as a positive control, the anti–plexin B1 antibody was independently verified by staining human skin (Supplementary Fig. S10).

Analyses of published data sets. The ONCOMINE 2.0 database (25)[7] was used as an interface to access published breast cancer microarray data sets. These data sets were analyzed for differential expression of plexin B1 among the class distinctions stored in the ONCOMINE database. The SymAtlas web application[8] was applied to analyze Affymetrix microarray data of normal human tissues stored in the SymGene database (26). Genome-wide gene expression data for 295 samples from the study of van de Vijver et al. (27) were downloaded from the website of Rosetta Inpharmatics.[9]

Statistical analysis. Subjects with missing values were excluded from the analyses and all reported P values were two sided. $P < 0.05$ was considered to indicate a significant result. For use as a binary variable, Affymetrix mRNA expression data of plexin B1 were categorized using a cutoff value of 500. In addition, a conservative procedure of median splitting was used for each independently analyzed sample group. Although it is also possible to use plexin B1 expression as a continuous prognostic factor, it is more appropriate and practical to group the tumors into two risk categories by use of a cutoff point when it is biologically meaningful, allowing, for example, direct comparison of Kaplan-Meier curves between groups. We chose the cutoff based on the expression level of plexin B1 in ER-negative tumors (see Results). This cutoff decision makes immediate biological sense because the gene was originally identified as a marker for ER-positive tumors, which display a behavior similar to that of ER-negative tumors. However, the results of the analyses did not change substantially when nearby cutoff points were used or plexin B1 levels were used in a continuous fashion (see Results). χ^2 test was used to test for associations between plexin B1 expression of tumors and standard clinical and molecular parameters. Survival intervals were measured from the time of surgery to the time of death from disease or of the first clinical or radiographic evidence of disease recurrence. Data for women in whom the envisaged end point was not reached were censored as of the last follow-up. We constructed Kaplan-Meier curves and used the log-rank test to determine the univariate significance of the variables. A Cox proportional hazards regression model was used to examine simultaneously the effects of multiple covariates on survival. The effect of each variable was assessed with the use of the Wald test and described by the hazard ratio with a 95% confidence interval. The stepwise Cox proportional hazards models initially included age, tumor size, lymph node status, molecular grading, ER, ErbB2, as well as plexin B1 expression. The final model was developed by dropping each variable in turn from the model and conducting a likelihood ratio test to compare the full and the nested models. A significance level of 0.1 as the cutoff to exclude a variable from the model was used. All analyses were done using SPSS 11.0 (SPSS, Inc., Chicago, IL).

Results

Plexin B1 expression in different human tissues and breast cancers. To gain further insight into the function of the *plexin B1* gene, we started our analysis with a survey of plexin B1 mRNA expression in various normal human tissues by using public available resources including the SymGene database (26). Plexin B1 expression was detected in a variety of human tissues (see Supplementary Fig. S5). Highest levels were observed in several regions of the brain, placenta, prostate, heart, colorectal adenocarcinoma, liver, lung, kidney, and thyroid, pointing to a role of plexin B1 in cells of ectodermal origin, which also constitute the progenitors of mammary epithelial cells. Furthermore, in previous microarray analyses of breast cancer samples, we and others identified *plexin B1* among genes that are most dependent on the ER status of the tumor (24), indicating an ER-driven regulation of plexin B1 in mammary epithelial cells.

Dysregulation of plexin B1 in ER-positive tumors. We have recently identified a subtype of breast cancers with stem cell–like features ("SCL" type) by gene expression profiling (28). A characteristic feature of those tumors was the perfect inverse correlation of ER expression and proliferative activity seen in this subgroup. In contrast, tumors that did not show this stem cell–like expression signature ("non-SCL" type) seemed to be frequently uncoupled from this tight link and displayed alterations in several ER-dependent transcriptional units, suggesting malfunctions in distinct branches of the ER regulatory network. The unique characteristic of SCL tumors allowed us to screen for altered expression in "uncoupled" tumors among 157 genes known to be dependent on the ER status. One of the genes that resulted from this screen was plexin B1, detected as part of a coregulated gene cluster containing a number of known genes involved in cellular adhesion. As shown in Supplementary Fig. S6, plexin B1 expression is strictly dependent on ER positivity but significantly reduced among those ER-positive samples in whom the proliferative activity was uncoupled from the ER status. In fact, *plexin B1* gene expression represents a link between those two vectors with a positive correlation to ER (*ESR1*) gene expression and a negative correlation to proliferative activity (see Supplementary Fig. S8). The correlation of plexin B1 expression with the ER status provides a clue for defining a reasonable cutoff point for Affymetrix microarray expression values of plexin B1. As presented in Fig. 1, only 2 of 40 (5%) ER-negative samples displayed an Affymetrix expression value >500 for plexin B1.

[7] http://www.oncomine.org
[8] http://symatlas.gnf.org/SymAtlas/
[9] http://www.rii.com/publications/2002/nejm.html

However, 27 of 79 (34%) of the ER-positive samples did show a negative result for plexin B1 when using this threshold.

Clinical characteristics of patients with plexin B1 expression. The clinical characteristics of patients with plexin B1 expression are presented in Table 1. Whereas we detected no correlation of tumor size and lymph node status with plexin B1 expression, a negative association with the age of the patient was observed. As stated above, a strong negative correlation of plexin B1 expression with the proliferative activity of the tumor was seen. Furthermore, plexin B1–expressing breast cancers are highly correlated with a lobular histology and a positive ER status, whereas ErbB2 was associated with low plexin B1 expression. These results are in line with low plexin B1 expression in the basal-like and ErbB2-like molecular subtypes when tumors were classified according to Sorlie et al. (19).

Loss of plexin B1 predicts poor outcome in ER-positive breast cancers. As shown in Fig. 2, plexin B1 displayed a significant prognostic value for disease-free survival. This effect was seen both in all patients (Fig. 2A) and in the ER-positive subgroup (Fig. 2B). In addition, plexin B1 seems to be of prognostic value in patients with a negative as well as a positive lymph node status (Fig. 2C and D, respectively) and independent of the type of chemotherapy used (epirubicin-cyclophosphamide or cyclophosphamide-methotrexate-5-fluorouracil; data not shown). Moreover, when comparing plexin B1 in univariate analysis to standard parameters, as denoted in Table 2, plexin B1 mRNA expression (Affymetrix value >500) displayed the highest prognostic value. This result was obtained for the whole sample group ($P = 0.0062$) as well as the subset of ER-positive patients ($P = 0.0107$). Even a very conservative approach of median splitting of plexin B1 Affymetrix values among each individual sample group resulted in high prognostic values ($P = 0.0173$ and $P = 0.0526$). Finally, as stated in Table 2, in a stepwise multivariable Cox regression model starting with all standard parameters, only plexin B1 ($P = 0.032$ and 0.022), tumor size ($P = 0.017$ and 0.026), and ErbB2 ($P = 0.048$ and 0.004) remained significant among all patients as well as ER-positive patients only. Here, it should be noted that the high prognostic value of ErbB2 among ER-positive patients is based only on 9 (11.4%) ErbB2-expressing tumors in this subgroup (see Table 2). Similar results were obtained when using log plexin B1 expression as a continuous variable in the Cox regression model ($P = 0.020$; hazard ratio, 0.33, 95% confidence interval, 0.13-0.84; for log of plexin B1 among ER-positive patients).

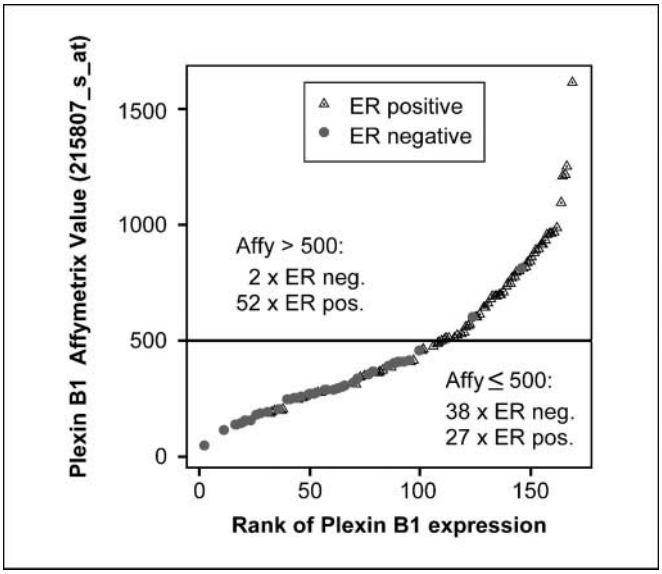

Fig. 1. Correlation of ER status and plexin B1 defines a threshold for plexin B1 Affymetrix expression values. Scatter plot of Affymetrix expression values of plexin B1 (probe set ID 215807_s_at) versus the rank of expression among 119 breast cancer samples. Triangles, ER-positive samples; gray dots, ER-negative samples. Horizontal line, Affymetrix expression value of 500, which was adopted as a biological threshold based on plexin B1 expression in ER-negative samples. The absolute numbers of ER-positive and ER-negative samples above and below this threshold are given.

Validation of plexin B1 mRNA expression by quantitative real-time PCR. Quantitative reverse transcription–based real-time PCR was used to validate the mRNA expression data obtained from the Affymetrix platform. Independent tissue samples were obtained from 29 of the tumors that were previously profiled on Affymetrix microarrays. Plexin B1 mRNA expression was measured using a SYBR green real-time PCR assay and the ΔC_t method was used to obtain relative expression values of plexin B1 as compared with GPDH. Both platforms display a highly significant correlation ($P = 0.001$). Supplementary Fig. S7 shows the box plot of ΔC_t values (plexin B1 versus GPDH) compared with qualitative data on plexin B1 expression as determined by microarray using >500 as cutoff value. From the plot, it can be deduced that this cutoff value roughly corresponds to a ΔC_t of ~ 5.

Prognostic value of plexin B1 expression can be verified on independent data sets. To verify our results on independent expression data, we analyzed published microarray data sets using the ONCOMINE database (25) as an interface. The data sets were investigated for differential expression of plexin B1 among the class distinctions stored in the ONCOMINE database. In line with our data, plexin B1 was dependent on the ER status in most studies (Supplementary Table S3). The highest significance ($P = 0.00005$) was obtained in the study of Wang et al. (29), which used the same Affymetrix microarray (HG-U133A) as in the work presented here. In addition, in three studies, a higher grading was correlated with reduced plexin B1 expression. Finally, reduced plexin B1 expression was correlated with early metastasis in the studies from the Netherlands Cancer Institute (27, 30). For a more detailed examination, we analyzed genome-wide gene expression data from van de Vijver et al. (27). The sample group was median split according to the expression value of the plexin B1 reporter (AB007867) on the microarray. As depicted in Fig. 3, plexin B1 expression showed a significant prognostic value both among all patients and in the ER-positive subgroup in this data set (Fig. 3A and B, respectively).

Plexin B1 protein is expressed by epithelial carcinoma cells. Recent observations (31, 32) suggested an additional function for plexin B1 in endothelial cells, and it was proposed that some carcinomas might exploit a proangiogenic effect of Sema4D as a chemoattractant on plexin B1–expressing endothelial cells (33). Accordingly, it could be speculated that expression of plexin B1 by the tumor cells themselves might sequester the secreted Sema4D and reduce its proangiogenic effect. In this case, the loss of plexin B1 would also be of

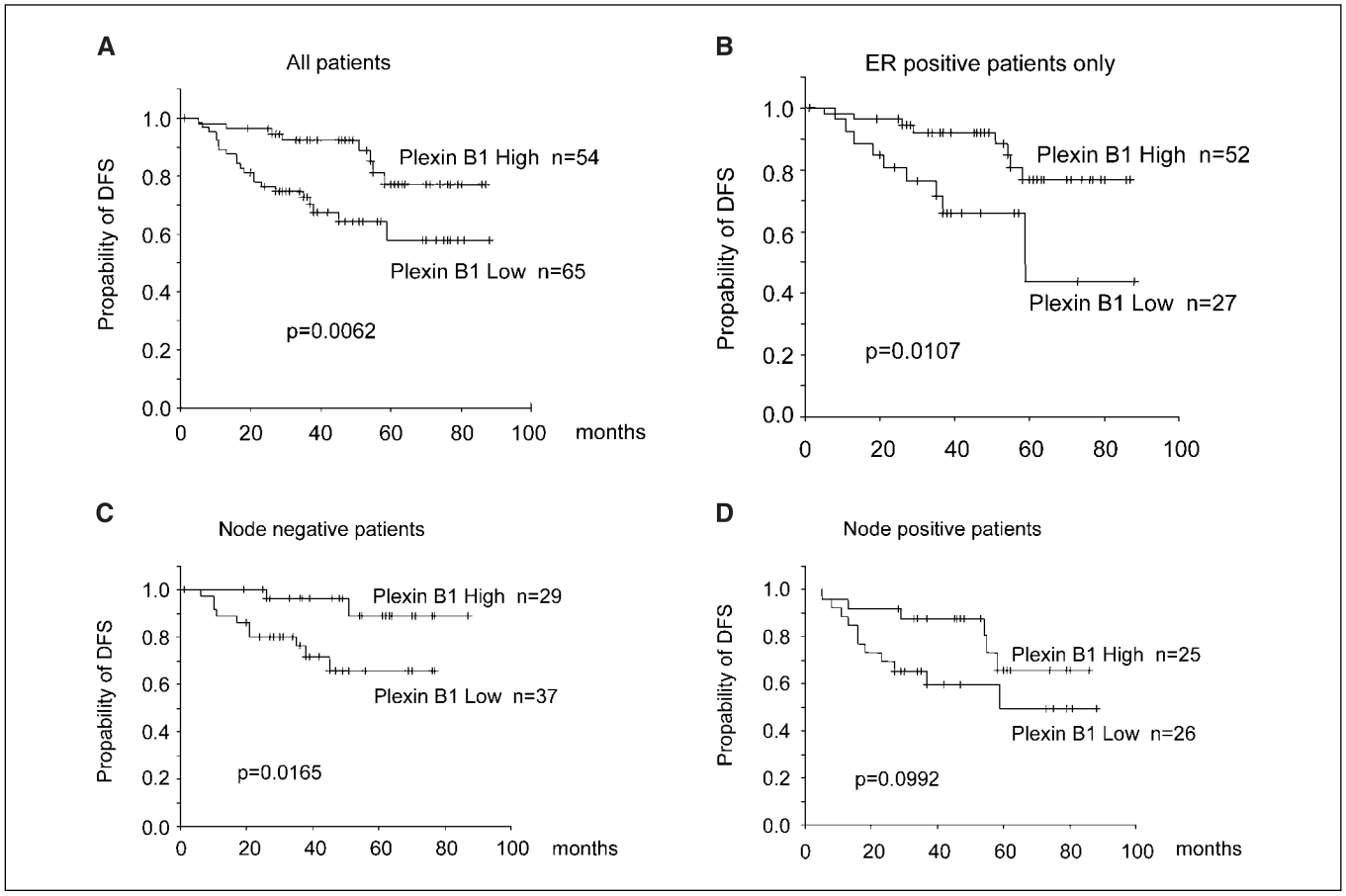

Fig. 2. Prognostic significance of loss of plexin B1 expression. Kaplan-Meier estimates of the disease-free survival of patients with tumors stratified by plexin B1 expression (Affymetrix threshold of 500) are given. Individual curves are presented for all patients (*A*), the ER-positive subgroup (*B*), all lymph node – negative patients (*C*), as well as lymph node – positive patients (*D*).

advantage for the tumor cells. In light of these different possibilities, a critical question is whether the tumor cells themselves or endothelial cells are the major source of plexin B1 expression in the tumor. Thus, we carried out immunohistochemistry to detect plexin B1 protein in those breast cancer samples with high *plexin B1* gene expression. As shown in Fig. 4 and Supplementary Fig. S4, expression of plexin B1 was detectable in ductal mammary epithelial cells.

Table 2. Univariate and multivariate analyses of standard parameters and plexin B1 in relation to disease-free survival

Parameter	All patients (*N* = 119)		ER-positive patients only (*n* = 79)	
Univariate analysis	*P*	*n*	*P*	*n*
Age (≤50 vs >50 y)	0.3129	59 vs 60	0.2731	44 vs 35
Tumor size (>2 vs ≤2 cm)	0.0232	59 vs 60	0.0747	39 vs 40
Lymph node (positive vs negative)	0.1308	51 vs 66	0.1139	39 vs 39
Molecular grading (above vs below median proliferation)	0.0395	60 vs 59	0.0872	39 vs 40
ER status (negative vs positive)	0.1653	40 vs 79	n.a.	n.a.
HER2 mRNA (Affymetrix value >4,500 vs ≤4,500)	0.0690	23 vs 96	0.0121	9 vs 70
Plexin B1 mRNA median (below vs above median Affymetrix-value in each individual sample group)	0.0173	60 vs 59	0.0526	40 vs 39
Plexin B1 mRNA (Affymetrix value ≤500 vs >500)	0.0062	65 vs 54	0.0107	27 vs 52
Multivariate Cox regression	*P*	Hazard ratio (95% CI)	*P*	Hazard ratio (95% CI)
Tumor size (≤2 vs >2 cm)	0.017	0.35 (0.15-0.83)	0.026	0.25 (0.08-0.85)
Plexin B1 mRNA (Affymetrix-value >500 vs ≤500)	0.032	0.40 (0.17-0.93)	0.022	0.31 (0.12-0.85)
HER2 mRNA (Affymetrix value >4,500 vs ≤4,500)	0.048	2.41 (1.01-5.76)	0.004*	6.12 (1.81-20.7)*

*High hazard ratio based on only 9 (11.4%) HER2-expressing patients in this ER-positive subgroup.

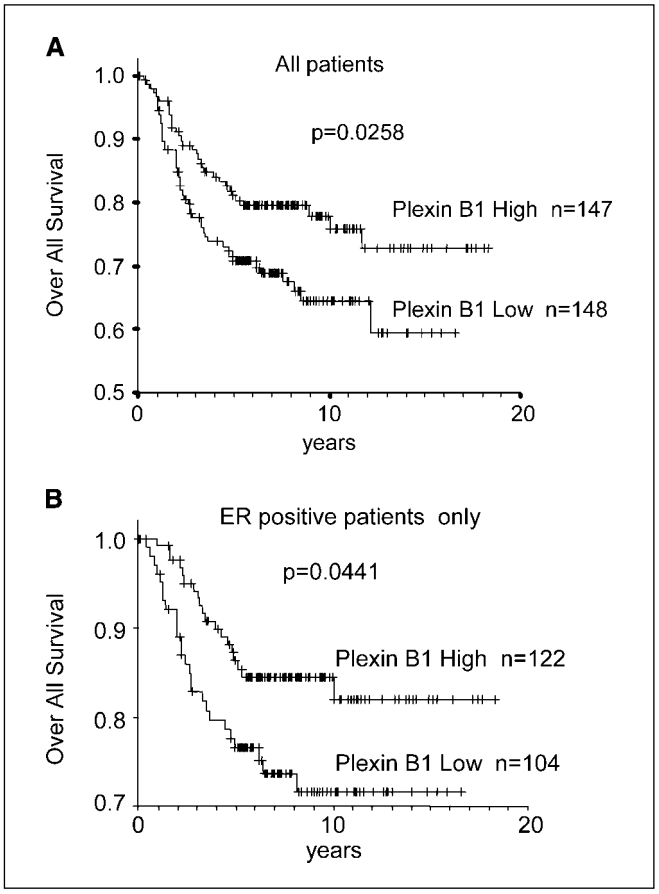

Fig. 3. Prognostic value of plexin B1 expression in published microarray data sets. The sample group of 295 breast tumors from the study of van de Vijver et al. (27) was median split according to the expression value of the plexin B1 reporter (AB007867) on their microarray. Kaplan-Meier estimates of survival of patients according to this stratification are given both for all patients (*A*) and the ER-positive subgroup (*B*).

Discussion

Using several complementing methods, we found that patients with breast cancers that are characterized by reduced plexin B1 expression display a poor prognosis. These results might suggest that plexin B1 suppress the invasive behavior of the tumor. However, the precise function of plexin B1 in tumors is not yet clear. On one hand, it was shown that plexin B1 couples with the receptor tyrosine kinases Met (3) and ErbB2 (14), and in both cases, Sema4D stimulates receptor kinase activity. This led researchers to speculate that the plexin B1-Met interaction may trigger invasive growth of epithelial cells by regulating MET signaling through its effectors like Grb2, Src, or phosphatidylinositol 3-kinase and the mitogen-activated protein kinase pathway (3). On the other hand, the semaphorins are well known as repellants defining areas of exclusion for plexin- and neuropilin-expressing neurons in the developing nervous system (34, 35). Both plexin A1 and plexin B1 signal repulsion when activated by their semaphorin ligands. Analogous to governing the repulsive growth of neurons, plexin D1 and Sema3E are required for the exclusion of vasculature from somites during development. Sema3E is expressed by the somites and functions as a stop sign for plexin D1–expressing endothelial cells, preventing vessels to colonize the somites (36). Consistently, Sema4D signaling through plexin B1 in the breast carcinoma cell line SKBR3 inhibits cell migration (37). The discovery that plexins have intrinsic GTPase-activating protein activity toward R-Ras (38) provided a link between the various aspects of semaphorin biology, suggesting that many of their effects relate to the plexin-mediated regulation of integrins by R-Ras. The repellent effect to turn away from the semaphorin source can thus be explained by R-Ras–mediated disruption of integrin binding to the extracellular matrix by semaphorin-plexin engagement on one side of the cell. An increased integrin binding to extracellular matrix on the opposing side where no semaphorin plexin interaction occurs leads to growth and migration. Thus, it has been suggested that any activation of plexin signaling might suppress metastasis by activating the GTPase-activating protein activity of plexins toward R-Ras, leading to decreased integrin binding. R-Ras is itself oncogenic (39–41). Constitutively active R-Ras has been found to increase cell migration of T47D breast epithelial cells (42) and cervical epithelial C33A cells (39) toward collagen. Consequently,

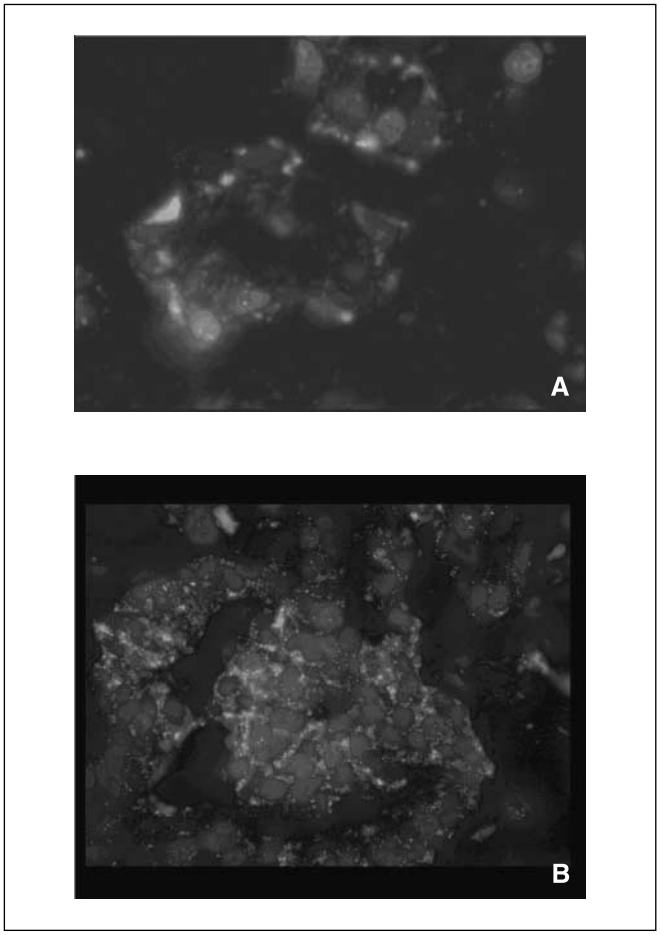

Fig. 4. Detection of plexin B1 protein on tumor cells. Plexin B1 protein was detected in 5-μm sections of tumor tissue from a breast cancer patient using a monoclonal antibody directed against plexin B1 and visualized with a Cy3-labeled secondary antibody. 4′,6-Diamidino-2-phenylindole was used to counterstain the nuclei of cells. *A,* normal mammary epithelial cells; *B,* tumor cells of an invasive ductal mammary carcinoma. No staining was seen when mammary carcinomas without plexin B1 mRNA expression were analyzed (data not shown). A color version of this figure is available online in Supplementary data (Suppl. Fig. S4).

semaphorin-stimulated plexin GTPase-activating protein activity might decrease cell migration in certain cancers. In conclusion, loss of plexin B1 expression could allow tumor cells to grow in opposite direction toward a repelling semaphorin gradient. This feature could promote an invasive behavior and enhance the distortion of normal tissue structure by the tumor cells. Our data emphasize that loss of plexin B1 characterizes a more aggressive tumor phenotype because low plexin B1 expression levels are associated with an impaired prognosis of breast cancer patients in both univariate (all patients, $P = 0.0062$; ER positive, $P = 0.0107$) and multivariate (all patients, $P = 0.032$; ER positive, $P = 0.022$) analyses, outperforming standard prognostic parameters such as tumor size, nodal status, ER status, etc. This observation is not only confined to our study cohort but can also be verified in microarray analyses of several authors, underlining the validity of our findings. Furthermore, differential expression of plexin B1 was validated by PCR analysis confirming the results of our microarray data.

Factors that are regulatorily involved in expression of plexin B1 are largely unknown. Here, we can show that plexin B1 expression is strongly correlated with expression of ER and low proliferative state of mammary carcinoma cells (see Supplementary Fig. S8). Yet loss of plexin B1 expression was observed in the subset of ER-positive tumors with high proliferation (uncoupled tumors), contrasting the normal inverse relationship between the ER status and the proliferative activity of the tumor (43, 44). When classifying tumors according to the intrinsic gene set described by Sorlie et al., the loss of plexin B1 is mainly confined to the basal-like and ErbB2-like tumors. However, roughly one third of all luminal A tumors show a low plexin B1 expression ≤ 500 (see Table 1).

Recent results (31, 32) also propose an additional function for plexin B1 in endothelial cells. Here, Sema4D promotes endothelial cell migration and tubulogenesis *in vitro* and the formation of blood vessels *in vivo*. A new study (33) even suggested that head and neck squamous cell carcinomas and other epithelial-derived tumors, including breast carcinomas, might indeed exploit the proangiogenic effect of Sema4D to promote tumor growth and survival and enhance their metastatic potential. In this scenario, Sema4D would be a chemoattractant rather than a repellent for plexin B1–expressing endothelial cells. Accordingly, it could be speculated that expression of plexin B1 by the tumor cells themselves might sequester the secreted Sema4D and reduce its proangiogenic effect. In this case, the loss of plexin B1 would also be of advantage for the tumor cells. Thus, an important aspect of our results is the immunohistochemical demonstration that the tumor cells themselves and not the endothelial cells are the major source of plexin B1 expression in the tumor.

In conclusion, plexin B1 represents an important new prognostic marker for breast cancer. Moreover, because of the normal inverse link between ER status and proliferation seen in plexin B1–expressing tumors, loss of plexin B1 might also act as a predictive marker indicating an endocrine resistance. The use of estrogen and progesterone receptor status to select for endocrine therapy is undeniably crucial. However, novel markers of a functional ER signaling like plexin B1 may also predict response to endocrine therapy as has been suggested for ErbB2 (45). To evaluate this potential role of plexin B1, further clinical investigations should be done.

Acknowledgments

We thank Katherina Kourtis for expert technical assistance.

References

1. Kruger RP, Aurandt J, Guan KL. Semaphorins command cells to move. Nat Rev Mol Cell Biol 2005;6:789–800.
2. Bussolino F, Valdembri D, Caccavari F, Serini G. Semaphoring vascular morphogenesis. Endothelium 2006;13:81–91.
3. Giordano S, Corso S, Conrotto P, et al. The semaphorin 4D receptor controls invasive growth by coupling with Met. Nat Cell Biol 2002;4:720–4.
4. Behar O, Golden JA, Mashimo H, Schoen FJ, Fishman MC. Semaphorin III is needed for normal patterning and growth of nerves, bones and heart. Nature 1996;383:525–8.
5. Gitler AD, Lu MM, Epstein JA. PlexinD1 and semaphorin signaling are required in endothelial cells for cardiovascular development. Dev Cell 2004;7:107–16.
6. Torres-Vazquez J, Gitler AD, Fraser SD, et al. Semaphorin-plexin signaling guides patterning of the developing vasculature. Dev Cell 2004;7:117–23.
7. Kagoshima M, Ito T. Diverse gene expression and function of semaphorins in developing lung: positive and negative regulatory roles of semaphorins in lung branching morphogenesis. Genes Cells 2001;6:559–71.
8. Morris JS, Stein T, Pringle MA, et al. Involvement of axonal guidance proteins and their signaling partners in the developing mouse mammary gland. J Cell Physiol 2006;206:16–24.
9. Takegahara N, Takamatsu H, Toyofuku T, et al. Plexin-A1 and its interaction with DAP12 in immune responses and bone homeostasis. Nat Cell Biol 2006;8:615–22.
10. Tse C, Xiang RH, Bracht T, Naylor SL. Human semaphorin 3B (SEMA3B) located at chromosome 3p21.3 suppresses tumor formation in an adenocarcinoma cell line. Cancer Res 2002;62:542–6.
11. Xiang R, Davalos AR, Hensel CH, Zhou XJ, Tse C, Naylor SL. Semaphorin 3F gene from human 3p21.3 suppresses tumor formation in nude mice. Cancer Res 2002;62:2637–43.
12. Brambilla E, Constantin B, Drabkin H, Roche J. Semaphorin SEMA3F localization in malignant human lung and cell lines: a suggested role in cell adhesion and cell migration. Am J Pathol 2000;156:939–50.
13. Bielenberg DR, Hida Y, Shimizu A, et al. Semaphorin 3F, a chemorepulsant for endothelial cells, induces a poorly vascularized, encapsulated, nonmetastatic tumor phenotype. J Clin Invest 2004;114:1260–71.
14. Swiercz JM, Kuner R, Offermanns S. Plexin B1/RhoGEF-mediated RhoA activation involves the receptor tyrosine kinase ErbB-2. J Cell Biol 2004;165:869–80.
15. Modlich O, Prisack HB, Munnes M, Audretsch W, Bojar H. Predictors of primary breast cancers responsiveness to preoperative epirubicin/cyclophosphamide-based chemotherapy: translation of microarray data into clinically useful predictive signatures. J Transl Med 2005;3:32.
16. Eisen MB, Spellman PT, Brown PO, Botstein D. Cluster analysis and display of genome-wide expression patterns. Proc Natl Acad Sci U S A 1998;95:14863–8.
17. Foekens JA, Atkins D, Zhang Y, et al. Multicenter validation of a gene expression-based prognostic signature in lymph node-negative primary breast cancer. J Clin Oncol 2006;24:1665–71.
18. Gruvberger S, Ringner M, Chen Y, et al. Estrogen receptor status in breast cancer is associated with remarkably distinct gene expression patterns. Cancer Res 2001;61:5979–84.
19. Sorlie T, Perou CM, Tibshirani R, et al. Gene expression patterns of breast carcinomas distinguish tumor subclasses with clinical implications. Proc Natl Acad Sci U S A 2001;98:10869–74.
20. Rody A, Karn T, Gatje R, et al. Gene expression profiles of breast cancer obtained from core-cut biopsies before neoadjuvant docetaxel, Adriamycin, and cyclophoshamide chemotherapy correlate with routine prognostic markers and could be used to identify predictive signatures. Zentralbl Gynakol 2006;128:76–81.
21. Sotiriou C, Wirapati P, Loi S, et al. Gene expression profiling in breast cancer: understanding the molecular basis of histologic grade to improve prognosis. J Natl Cancer Inst 2006;98:262–72.
22. Holtrich U, Wolf G, Brauninger A, et al. Induction and down-regulation of PLK, a human serine/threonine kinase expressed in proliferating cells and tumors. Proc Natl Acad Sci U S A 1994;91:1736–40.
23. Ahr A, Holtrich U, Solbach C, et al. Molecular classification of breast cancer patients by gene expression profiling. J Pathol 2001;195:312–20.
24. Ahr A, Karn T, Solbach C, et al. Identification of high risk breast-cancer patients by gene expression profiling. Lancet 2002;359:131–2.
25. Rhodes DR, Yu J, Shanker K, et al. ONCOMINE: a cancer microarray database and integrated data-mining platform. Neoplasia 2004;6:1–6.
26. Su AI, Wiltshire T, Batalov S, et al. A gene atlas of the mouse and human protein-encoding transcriptomes. Proc Natl Acad Sci U S A 2004;101:6062–7.

27. van de Vijver MJ, He YD, van't Veer LJ, et al. A gene-expression signature as a predictor of survival in breast cancer. N Engl J Med 2002;347:1999–2009.

28. Rody A, Holtrich U, Müller V, et al. c-kit: identification of co-regulated genes by gene expression profiling and clinical relevance of two breast cancer subtypes with stem cell like features. 2006 ASCO Annual Meeting Proceedings Part I. J Clin Oncol 2006;24:622.

29. Wang Y, Klijn JG, Zhang Y, et al. Gene-expression profiles to predict distant metastasis of lymph-node-negative primary breast cancer. Lancet 2005;365:671–9.

30. van't Veer LJ, Dai H, van de Vijver MJ, et al. Gene expression profiling predicts clinical outcome of breast cancer. Nature 2002;415:530–6.

31. Basile JR, Barac A, Zhu T, Guan KL, Gutkind JS. Class IV semaphorins promote angiogenesis by stimulating Rho-initiated pathways through plexin B. Cancer Res 2004;64:5212–24.

32. Conrotto P, Valdembri D, Corso S, et al. Sema4D induces angiogenesis through Met recruitment by plexin B1. Blood 2005;105:4321–9.

33. Basile JR, Castilho RM, Williams VP, Gutkind JS. Semaphorin 4D provides a link between axon guidance processes and tumor-induced angiogenesis. Proc Natl Acad Sci U S A 2006;103:9017–22.

34. Fiore R, Puschel AW. The function of semaphorins during nervous system development. Front Biosci 2003;8:S484–99.

35. Huber AB, Kolodkin AL, Ginty DD, Cloutier JF. Signaling at the growth cone: ligand-receptor complexes and the control of axon growth and guidance. Annu Rev Neurosci 2003;26:509–63.

36. Gu C, Yoshida Y, Livet J, et al. Semaphorin 3E and plexin-D1 control vascular pattern independently of neuropilins. Science 2005;307:265–8.

37. Barberis D, Artigiani S, Casazza A, et al. Plexin signaling hampers integrin-based adhesion, leading to Rho-kinase independent cell rounding, and inhibiting lamellipodia extension and cell motility. FASEB J 2004;18:592–4.

38. Oinuma I, Ishikawa Y, Katoh H, Negishi M. The semaphorin 4D receptor plexin B1 is a GTPase activating protein for R-Ras. Science 2004;305:862–5.

39. Rincon-Arano H, Rosales R, Mora N, Rodriguez-Castaneda A, Rosales C. R-Ras promotes tumor growth of cervical epithelial cells. Cancer 2003;97:575–85.

40. Yu Y, Feig LA. Involvement of R-Ras and Ral GTPases in estrogen-independent proliferation of breast cancer cells. Oncogene 2002;21:7557–68.

41. Cox AD, BrtvaTR, Lowe DG, Der CJ. R-Ras induces malignant, but not morphologic, transformation of NIH3T3 cells. Oncogene 1994;9:3281–8.

42. Keely PJ, Rusyn EV, Cox AD, Parise LV. R-Ras signals through specific integrin α cytoplasmic domains to promote migration and invasion of breast epithelial cells. J Cell Biol 1999;145:1077–88.

43. Silverstrini R, Daidone MG, Di Fronzo G. Relationship between proliferative activity and estrogen receptors in breast cancer. Cancer 1979;44:665–70.

44. Jiang SY, Jordan VC. Growth regulation of estrogen receptor-negative breast cancer cells transfected with complementary DNAs for estrogen receptor. J Natl Cancer Inst 1992;84:580–91.

45. Pritchard KI. Endocrine therapy of advanced disease: analysis and implications of the existing data. Clin Cancer Res 2003;9:460–7S.

Supplementary Material:

Supplementary Figure 1: Correlation of estrogen receptor status and Plexin B1 defines a threshold for Plexin B1 Affymetrix expression values

Scatter plot of Affymetrix expression values of Plexin B1 (probe set ID 215807_s_at) vs. the rank of expression among 119 breast cancer samples. Estrogen receptor positive samples are represented by blue dots while ER negative samples shown as red dots. The horizontal line and shaded region represents the Affymetrix expression value of 500 which was adopted as a biological threshold based on Plexin B1 expression in ER negative samples. The absolute numbers of ER positive and negative samples above and below this threshold is given.

Supplementary Figure 4: Detection of Plexin B1 protein on tumor cells

Plexin B1 protein was detected in 5 µm sections of tumor tissue from a breast cancer patient using a monoclonal antibody directed against Plexin B1 and visualized using a Cy3 labeled secondary antibody (red staining). DAPI was used to counterstain the nuclei of cells (blue staining). **A:** normal mammary epithelial cells, **B:** tumor cells of an invasive ductal mammary carcinoma. No staining was seen when mammary carcinoma without Plexin B1 mRNA expression were analyzed (data not shown).

Supplementary Figure 5: Plexin B1 gene expression among different normal tissues

Affymetrix microarray data of Plexin B1 (probe set ID 215807_s_at) expression in 79 human tissues were retrieved from the SymGene database (http://symatlas.gnf.org/SymAtlas/) and represented as bar chart. Median, threefold and tenfold median values are represented by black, blue and red lines, respectively.

Supplementary Figure 6: Plexin B1 is dysregulated among "uncoupled" breast cancers

Box plot of Affymetrix expression values of Plexin B1 (probe set ID 215807_s_at) in different sample groups. Samples are stratified as stem cell like (SCL) and Non-SCL breast cancers and by their estrogen receptor status. Among ER positive Non-SCL tumors those with a normal coupling between receptor status and proliferation are separated from the "uncoupled" tumors ("ER^+ unc.").

Supplementary Figure 7: Validation of Plexin B1 expression by quantitative Real-Time PCR

Reverse transcription based Real Time PCR was performed on 29 independent tissue samples from tumors which were profiled before on Affymetrix microarrays. Box plots of Δc_t values (Plexin B1 vs. GPDH) are given and samples stratified by the Plexin B1 expression value on the Affymetrix platform.

Supplementary Figure 8: Multidimensional scaling of Plexin B1 vs. ESR1 and proliferation

All 119 breast cancer samples were ranked according to their Affymetrix expression values of Plexin B1 (215807_s_at), ESR1 (205225_at), and their proliferative activity based on the cluster of 136 proliferation associated genes. Tumor samples were then placed in a three dimensional scatter plot according to these ranks and a surface visualisation was obtained by using local linear regression as a smoother with a normal kernel and a bandwith of 3.0.

Supplementary Figure 9: Analysis of the proliferation state of breast cancer samples

A cluster of 136 highly correlated genes well known for their association with proliferation was used to obtain a robust quantitative metric of the proliferation. Each marker was median centered over all samples, subsequently the median expression of all marker determined for each sample and finally as an ordinal variable all samples ranked according this proliferation metric from left to right. The 136 applied probe sets are listed in Suppl. Table 4.

Supplementary Figure 10: Detection of Plexin B1 protein in normal human skin tissue

Plexin B1 protein was detected in 15 µm sections of normal skin tissue using a monoclonal antibody directed against Plexin B1 and visualized using a Cy3 labeled secondary antibody (red staining). IHC was performed as described for the detection of Plexin B1 in breast cancer samples. The epidermis including str. corneum, str. spinosum and str. basale are positive for Plexin B1 protein expression. No staining was observed in the dermis.

Supplementary Table 3: Differential expression of Plexin B1 according to published microarray datasets

Supplementary Table 4: Genes applied for proliferation metric

List of the 136 highly correlated proliferation associated probe sets used for the analysis of proliferative state of samples in Supplementary Figure 9.

Figure 1: Correlation of estrogen receptor status and Plexin B1 defines a threshold for Plexin B1 Affymetrix expression values

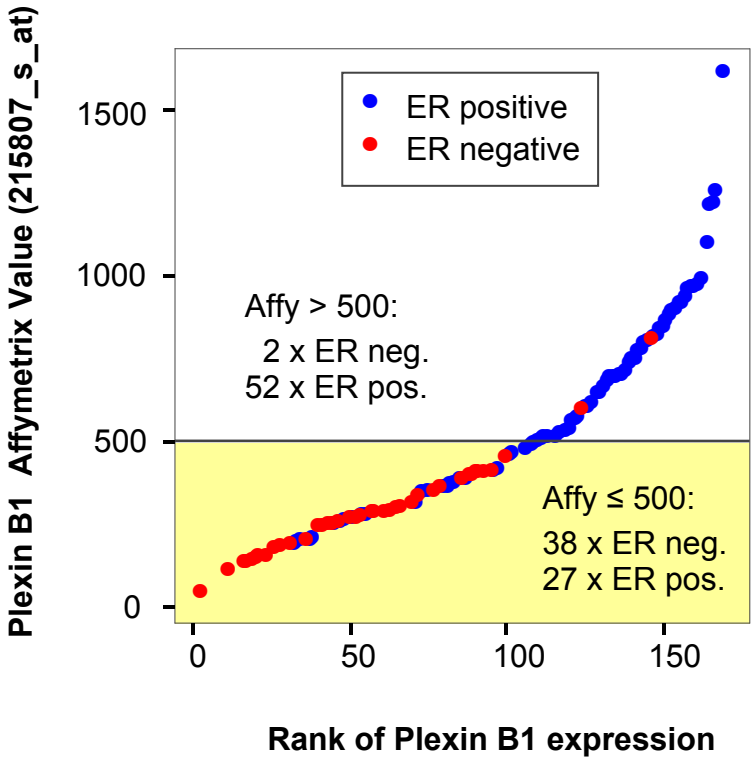

Supplementary Figure 4: Detection of Plexin B1 protein on tumor cells

A.

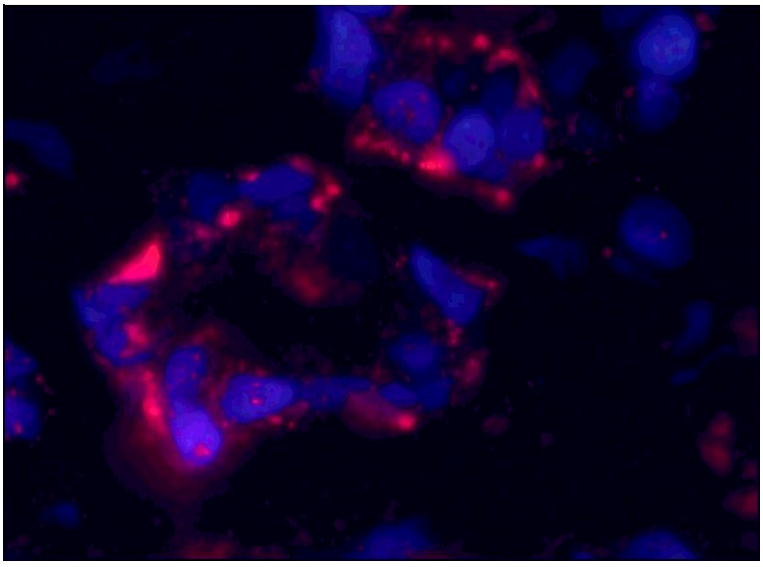

B.

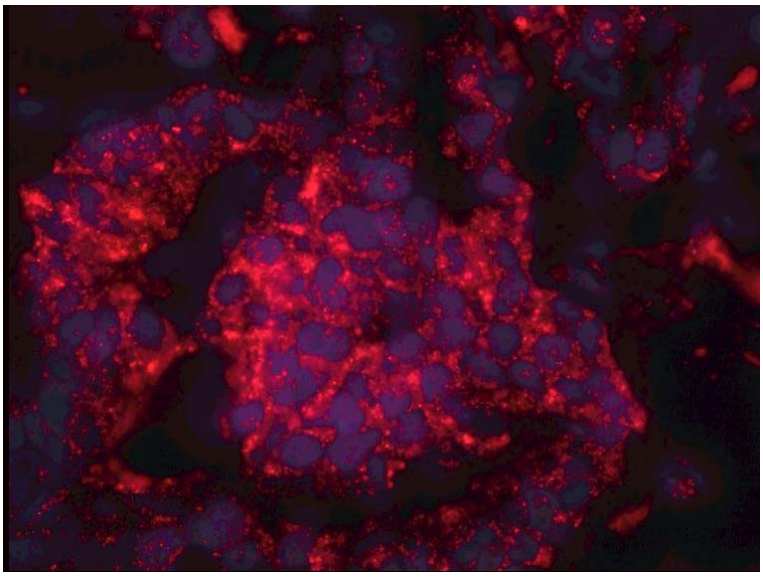

Supplementary Figure 5: Plexin B1 gene expression among different normal tissues

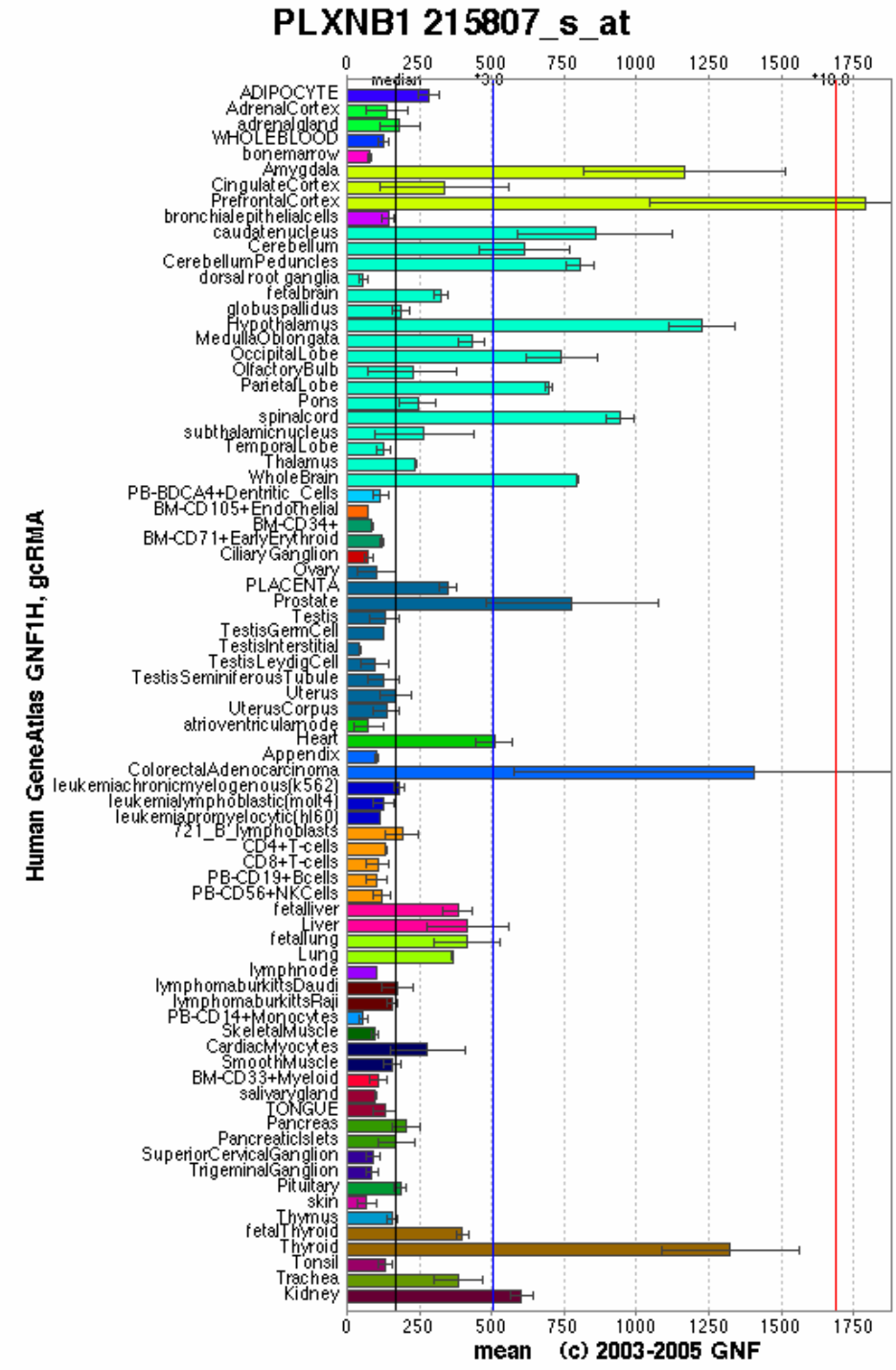

Supplementary Figure 6: Plexin B1 is dysregulated among "uncoupled" breast cancers

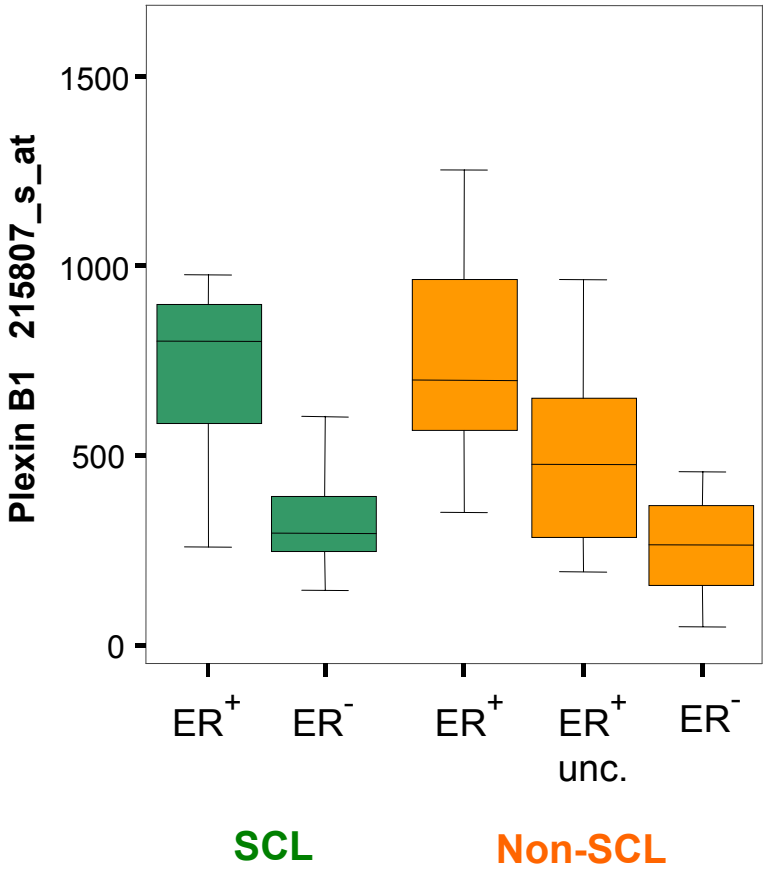

Supplementary Figure 7: Validation of Plexin B1 expression by quantitative Real-Time PCR

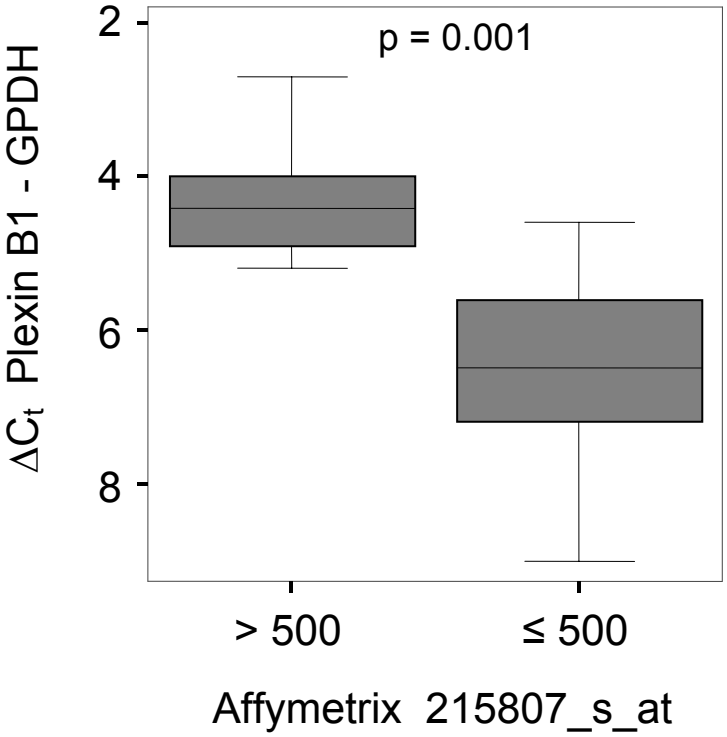

Supplementary Figure 8: Scatter plot of Plexin B1 vs. ESR1 and proliferation

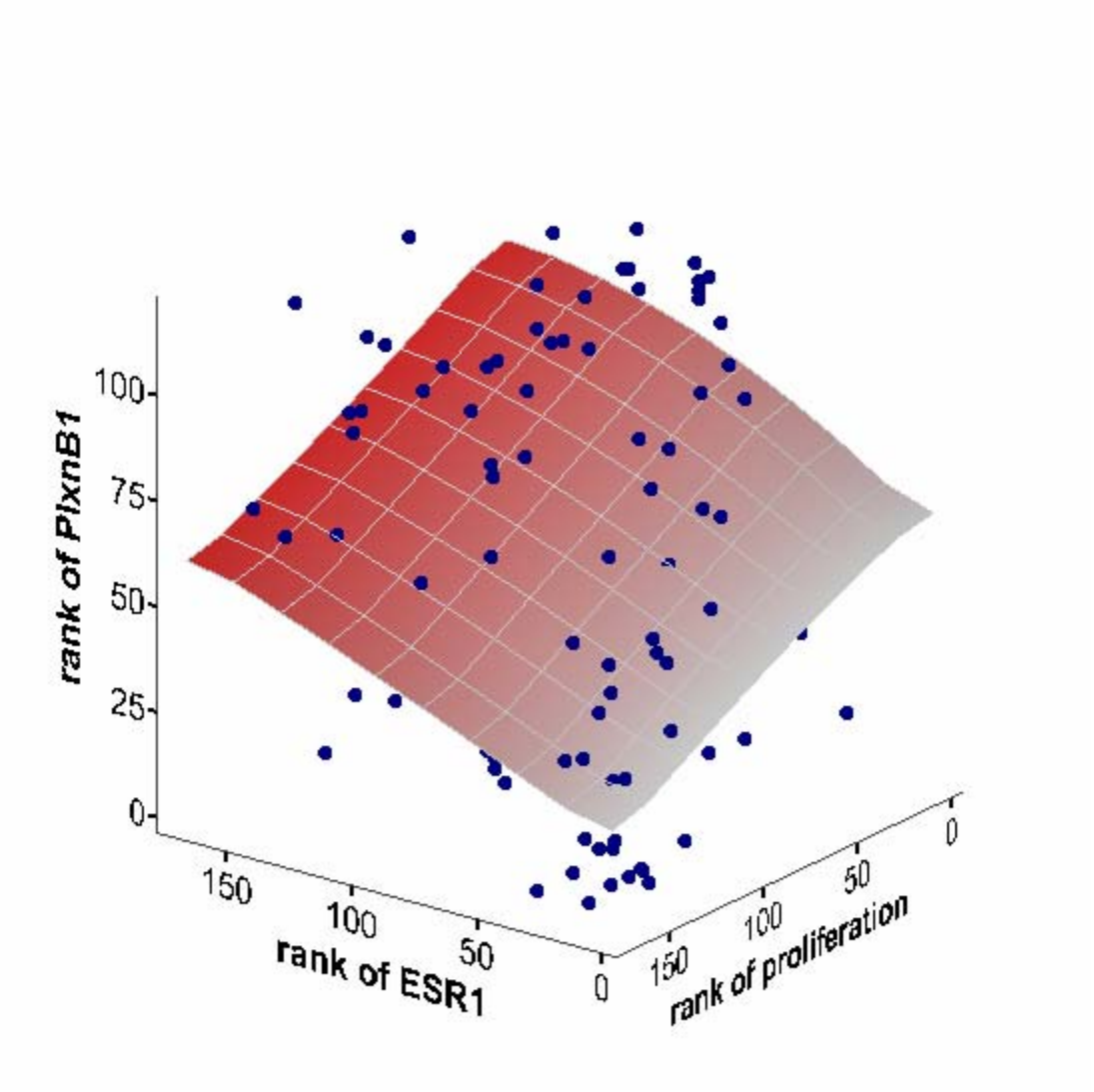

Supplementary Figure 9: Analysis of the proliferation state of breast cancer samples

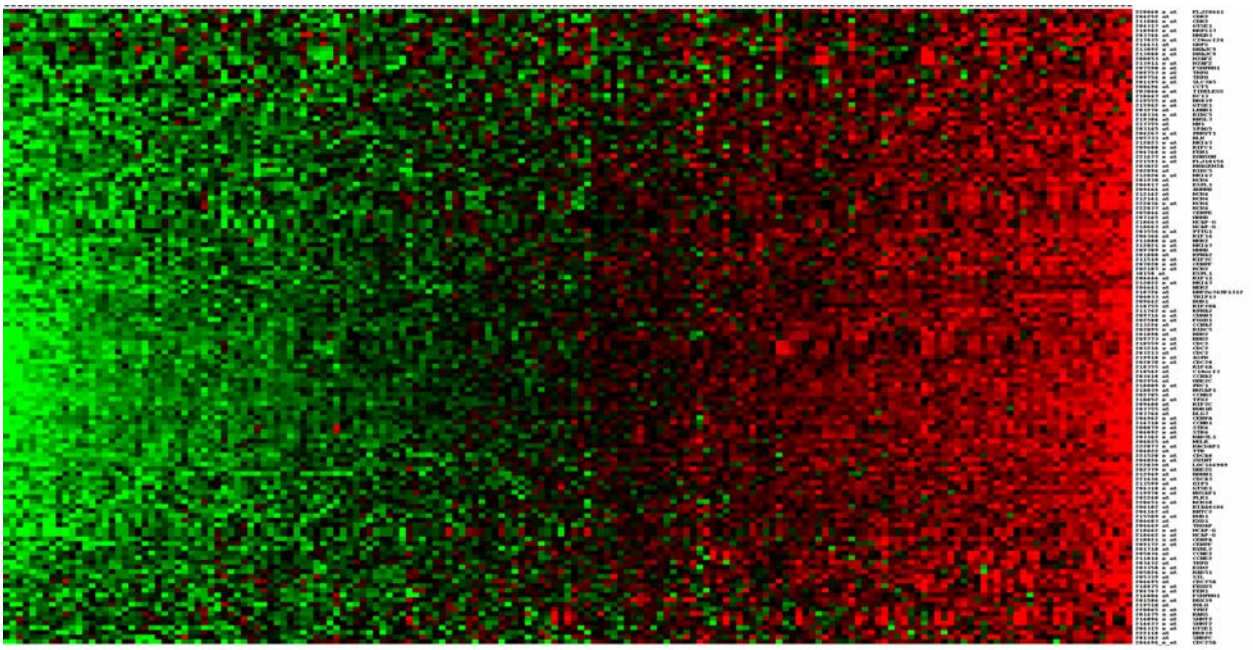

Supplementary Figure 10: Detection of Plexin B1 protein in human skin tissue

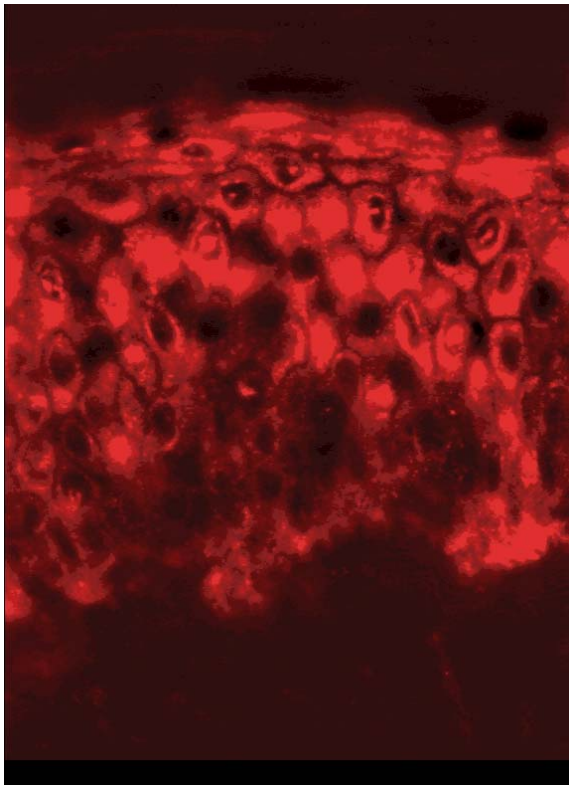

Epidermis

Dermis

Supplementary Table 3: Differential expression of Plexin B1 according to published microarray datasets

Classes	Study	Platform	Reporter	Test	p-value
ER status	Wang et al.	Affymetrix U133A	215807_s_at	T-Test	0.00005
ER status	van de Vijver et al.	Inkjet spotted oligos	AB007867	T-Test	0.003
ER status	Zhao et al.	spotted cDNA	IMAGE:2541458	T-Test	0.017
ER status	Gruvberger et al.	spotted cDNA	IMAGE:755952	T-Test	0.035
ER status	Sotiriou et al. 2003	spotted cDNA	IMAGE:755952	T-Test	0.110
ER status	Sorlie et al. 2003	spotted cDNA	IMAGE:755952	T-Test	0.800
ER status	West et al.	Affymetrix HuGeFL	X87904_at	T-Test	0.310
Grade 2 vs 3	Perou et al.	spotted cDNA	IMAGE:755952	T-Test	0.018
Grade	Sotiriou et al. 2003	spotted cDNA	IMAGE:755952	T-Test	0.032
Grade	Sorlie et al. 2003	spotted cDNA	IMAGE:755952	T-Test	0.082
Metastasis within 5 yr	van t'Veer et al.	Inkjet spotted oligos	AB007867	T-Test	0.011
Metastasis within 5 yr	van de Vijver et al.	Inkjet spotted oligos	AB007867	T-Test	0.035
ER+ Metast. within 5 yr	van de Vijver et al.	Inkjet spotted oligos	NM_002673	T-Test	0.144
No Metastasis	van t'Veer et al.	Inkjet spotted oligos	AB007867	Cox-Regr.	0.006
Survival	van de Vijver et al.	Inkjet spotted oligos	AB007867	Cox-Regr.	0.024

Supplementary Table 4: Genes applied for proliferation metric

Affymetrix probe set	Gene Symbol
219918_s_at	ASPM
209464_at	AURKB
210334_x_at	BIRC5
202094_at	BIRC5
202095_s_at	BIRC5
205733_at	BLM
219555_s_at	BM039
222118_at	BM039
212949_at	BRRN1
209642_at	BUB1
215509_s_at	BUB1
203755_at	BUB1B
218542_at	C10orf3
217835_x_at	C20orf24
213226_at	CCNA2
203418_at	CCNA2
214710_s_at	CCNB1
202705_at	CCNB2
205034_at	CCNE2
211814_s_at	CCNE2
208696_at	CCT5
210559_s_at	CDC2
203214_x_at	CDC2
203213_at	CDC2
202870_s_at	CDC20
204695_at	CDC25A
204696_s_at	CDC25A
221436_s_at	CDCA3
221520_s_at	CDCA8
204252_at	CDK2
211804_s_at	CDK2
209714_s_at	CDKN3
204962_s_at	CENPA
210821_x_at	CENPA
205046_at	CENPE
207828_s_at	CENPF
209172_s_at	CENPF
218447_at	DC13
201584_s_at	DDX39
218726_at	DKFZp762E1312
203764_at	DLG7
213092_x_at	DNAJC9
213088_s_at	DNAJC9
221677_s_at	DONSON
204817_at	ESPL1
38158_at	ESPL1
204603_at	EXO1
203358_s_at	EZH2
218875_s_at	FBXO5
204768_s_at	FEN1

Affymetrix probe set	Gene Symbol
204767_s_at	FEN1
221591_s_at	FLJ10156
220060_s_at	FLJ20641
202580_x_at	FOXM1
207590_s_at	FSHPRH1
214804_at	FSHPRH1
214431_at	GMPS
204317_at	GTSE1
215942_s_at	GTSE1
204318_s_at	GTSE1
204315_s_at	GTSE1
200853_at	H2AFZ
213911_s_at	H2AFZ
218663_at	HCAP-G
218663_at	HCAP-G
218662_s_at	HCAP-G
218662_s_at	HCAP-G
203744_at	HMGB3
207165_at	HMMR
209709_s_at	HMMR
217755_at	HN1
206102_at	KIAA0186
204444_at	KIF11
206364_at	KIF14
218755_at	KIF20A
211519_s_at	KIF2C
209408_at	KIF2C
218355_at	KIF4A
209680_s_at	KIFC1
219306_at	KNSL7
204162_at	KNTC2
201088_at	KPNA2
211762_s_at	KPNA2
203276_at	LMNB1
222039_at	LOC146909
203362_s_at	MAD2L1
201475_x_at	MARS
220651_s_at	MCM10
202107_s_at	MCM2
212142_at	MCM4
212141_at	MCM4
222036_s_at	MCM4
222037_at	MCM4
201930_at	MCM6
204825_at	MELK
212023_s_at	MKI67
212020_s_at	MKI67
212021_s_at	MKI67
212022_s_at	MKI67
218982_s_at	MRPS17

Affymetrix probe set	Gene Symbol
201710_at	MYBL2
211080_s_at	NEK2
204641_at	NEK2
218039_at	NUSAP1
219978_s_at	NUSAP1
213599_at	OIP5
204267_x_at	PKMYT1
202240_at	PLK1
219510_at	POLQ
218009_s_at	PRC1
203554_x_at	PTTG1
222077_s_at	RACGAP1
205024_s_at	RAD51
203022_at	RNASEH2A
201890_at	RRM2
209773_s_at	RRM2
214096_s_at	SHMT2
214437_s_at	SHMT2
205339_at	SIL
201195_s_at	SLC7A5
201342_at	SNRPC
203145_at	SPAG5
208079_s_at	STK6
204092_s_at	STK6
203046_s_at	TIMELESS
209753_s_at	TMPO
209754_s_at	TMPO
203432_at	TMPO
220865_s_at	TPRT
210052_s_at	TPX2
204033_at	TRIP13
204649_at	TROAP
204822_at	TTK
202954_at	UBE2C
202779_s_at	UBE2S
204026_s_at	ZWINT